Catalysis Today xxx (2014) xxx–xxx

Contents lists available at ScienceDirect

Catalysis Today

journal homepage: www.elsevier.com/locate/cattod

Fabrication of high-sensitivity palladium loaded tungsten trioxide photocatalyst by photodeposite method

Yuka Sakai*, Asami Shimanaka, Masahiko Shioi, Shigeru Kato, Shigeo Satokawa, Toshinori Kojima, Akihiro Yamasaki

Department of Materials and Life Sciences, Faculty of Science and Engineering, Seikei University, 3-3-1 Kichijoji-kitamachi, Musashino-shi, Tokyo 180-8633, Japan

ARTICLE INFO

Article history:
Received 15 February 2014
Received in revised form 4 July 2014
Accepted 25 July 2014
Available online xxx

Keywords:
Pollution treatment
Tungsten oxide
Visible light
Fluorescent lamp
Photocatalyst
Photodeposition

ABSTRACT

Pd-supported tungsten oxide (Pd/WO_3) was prepared by photodeposition by using black light. X-ray diffraction and X-ray photoelectron spectroscopy analyses of Pd/WO_3 confirmed the presence of Pd(0). Pd(0) was uniformly dispersed on the surface of WO_3. The optimum Pd amount for the degradation of aqueous methylene blue (MB) was 0.5 wt%, and the photocatalytic activity in this case was 27 times higher than that of pure WO_3. The optimum Pd amount for the decomposition of gaseous acetaldehyde was 0.1 wt%, and the photocatalytic activity using this amount of Pd was 5.9 times greater than that for pure WO_3. Pd as a support improved the charge separation efficiency. Further, hydrogen peroxide was produced on the Pd(0) side of the photocatalyst because of the movement of photoexcited electrons, and it contributed significantly to MB degradation. Moreover, electrons produced with MB moved to the Pd side, and contributed to hydrogen peroxide production. Only photocatalytic degradation contributed to acetaldehyde decomposition, while both photocatalytic and self-sensitized degradation contributed to MB degradation. The Pd/WO_3 sample containing the optimal amount of Pd acted as an effective photocatalyst, despite the difference between the optimal Pd amount required for acetaldehyde decomposition and that for MB degradation.

1. Introduction

Titanium dioxide (TiO_2) is a well-known photocatalyst that is widely used for the decomposition of volatile organic compounds (VOCs) and the environmental remediation of wastewater [1–6].

Now, anatase-type TiO_2 has high photocatalytic activity; however, its bandgap is 3.2 eV, as a result of which ultraviolet (UV) light is required for its photoexcitation. To realize increased applications, a photocatalyst that has good activity under visible light is required.

Therefore, some studies have attempted to modify TiO_2 through approaches such as metal ion implantation and anion doping to realize improved properties [7–17]. Others have investigated the bandgap structures of various semiconductor photocatalysts from the viewpoint of finding an alternative to TiO_2. Tungsten oxide (WO_3) has a bandgap of ~2.8 eV [18–21], and it is known to absorb light with a wavelength of 443 nm (visible light) or less. However, the lower edge of its conduction band is more positive than the reduction level of hydrogen. In addition, many photoexcited electrons recombine without using electrons for the reductive reaction. Therefore, the photoinduced redox reaction efficiency is low although WO_3 absorbs visible light.

Recently, many studies have focused on improving the photocatalytic activity of WO_3 by preparing metal-supported WO_3; in such catalysts, an increased number of holes are available because of the hydrogen peroxide generated on the support metal site and the improved charge segregation efficiency of the excited electrons [22–31].

The photocatalytic activity of platinum (Pt)-supported WO_3 prepared by the photodeposition method [23–26] using visible light has been reported to be comparable to that of TiO_2 (P25) for the vapor-phase decomposition of VOC under Xe lamp irradiation [23]. However, Pt is very expensive. Among studies attempting to produce more inexpensive catalysts, Arai et al. reported that WO_3 powder that was mechanically mixed with palladium (Pd) nanoparticles showed seven times the photocatalytic activity of nitrogen-doped TiO_2 under visible light irradiation [27]. In addition, Liu et al. reported the use of Pd-supported WO_3 powder (Pd/WO_3)

---

* Corresponding author. Tel.: +81 422 37 3020; fax: +81 422 37 3871.
E-mail addresses: yukaji_sakai1@yahoo.co.jp, sakai@ncassembly.jst.go.jp (Y. Sakai).

http://dx.doi.org/10.1016/j.cattod.2014.07.044

produced by a similar method for malachite green (MG) degradation [30]. The interfacial area of Pd/WO_3 obtained by this process is quite small.

In this study, a high-performance visible-light-responsive photocatalyst, Pd-loaded WO_3, was prepared by the photodeposition method using black light. The photocatalytic activity of this photocatalyst, which is referred to as Pd/WO_3, was investigated with respect to the degradation of aqueous methylene blue (MB), and the optimum Pd addition ratio for the highest activity was determined. The photocatalytic activity of Pd/WO_3 was further confirmed by using it for the decomposition of gaseous acetaldehyde.

We also evaluated the relationship between the Pd addition state and the photocatalytic activity of Pd/WO_3, and investigated the effectiveness of Pd/WO_3 that was prepared by the photodeposition method.

2. Experimental

2.1. Materials and sample preparation

WO_3 powder was supplied by Kojundo Chemical Laboratory, and Pd was obtained in the form of $PdCl_2$ from Wako. Pd-supported WO_3 powder (Pd/WO_3) was prepared by the photodeposition method using black light irradiation. The powder sample was then added to distilled water and mixed thoroughly. The resulting solution sample was dispersed by a supersonic wave and deaerated using Ar gas. $PdCl_2$ (wt.% vs. WO_3) was added to this solution, and Pd was deposited on the surface of WO_3 by black light (Toshiba Co., FL20SBLB) irradiation for 5 h at room temperature with stirring.

2.2. Characterization

XRD spectra of the prepared composite and single-component photocatalysts were measured in the measurement range of 20–60° by using a powder X-ray diffractometer (XRD, Rigaku Co., Ultima IV). UV spectra of the prepared samples were measured in the measurement range of 250–800 nm by using a UV–Visible (UV–Vis) spectrophotometer (Shimadzu Co., UV-3100 PC). The Brunauer–Emmett–Teller (BET) specific surface area of the prepared samples was measured by using a poresizer (Bel Japan Co., Belsorp-mini).

2.3. Dye degradation

Photocatalytic powder (1350 ppmw) was placed in a glass pail with MB solution (Kanto Co., Japan; 10 ppm) and dispersed in an ultrasound bath. It was then kept in the dark and agitated by using a magnetic stirrer for 20 h to evaluate the MB adsorption capacity of the photocatalyst. Then, it was irradiated using a fluorescent lamp (Toshiba Co., FLR40S·D-ED-D65/M) for 8 h under the same stirring conditions as those described above. During irradiation, 2 mL of the sample solution was collected at regular intervals and diluted by 5 times using distilled water. The light absorption of the sample solution was measured by using a UV–Vis spectrophotometer (Shimadzu Co., UV-1700) at the maximum absorption wavelength of MB of 665 nm. Degradation rate of the MB concentration assumed to the first-order reaction, and the photocatalytic activities were compared based on the reaction rate constant.

2.4. Decomposition of gaseous acetaldehyde

The photocatalytic activity of Pd/WO_3 with respect to the decomposition of gaseous acetaldehyde was investigated using a batch-type reactor and a 150 W Xe lamp equipped with a UV (<400 nm) cut-off filter. The gaseous acetaldehyde and the CO_2 produced during its decomposition were sampled, and their concentrations were measured using gas chromatography systems equipped with a flame ionization detector (GC-FID) (Shimadzu, GC-8A and GC-2014) and a methanizer (Shimadzu, MTN-1).

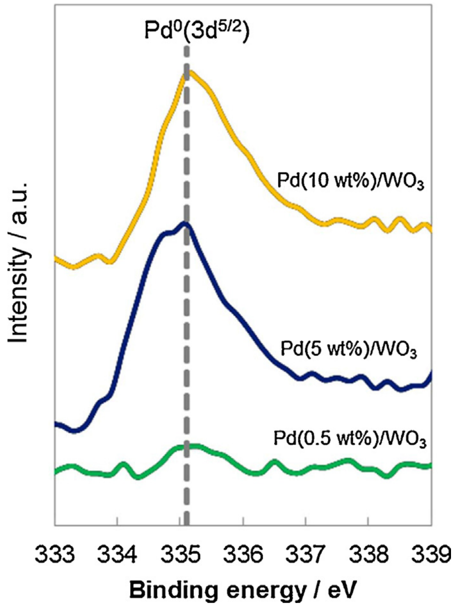

Fig. 1. XPS (Pd-3d) binding energies of the Pd/WO_3 photocatalysis prepared in different Pd addition rate.

3. Results and discussion

Using (ICP-AES), it was confirmed that the amount of Pd loaded was the same as the amount of Pd fed (Thermo Fisher SCIENTIFIC iCAP-6000 series).

The results of the X-ray photoelectron spectroscopy (XPS, PERKIN ELMER) analysis showed that almost all of the loaded Pd was in the zero-valence state (Fig. 1).

The X-ray diffractometer (XRD, Rigaku Co., Ultima IV) analysis results of all the samples are shown in Fig. 2. The circle denotes the monoclinic-phase peak attributable to WO_3 [32,33]. A peak attributable to the face-centered cubic (fcc) phase of Pd was noticed for an addition ratio of 5 wt%. This result shows that Pd/WO_3 contained a considerable amount of Pd(0). However, when the addition ratio was 1 wt% or lower, the peak attributable to Pd was not noticed.

Fig. 3 shows field-emission scanning electron microscope (FE-SEM, JEOL Ltd., JSM-7001F) images and the Pd elemental concentration maps for Pd(0.5 wt%)/WO_3 and Pd(5 wt%)/WO_3 (energy dispersive X-ray spectrometry: EDS, JED-2300F).

Pd(0) was dispersed uniformly on the surface of WO_3; however, the partial aggregation of Pd was also observed when the Pd addition ratio was high. In the case of the Pd/WO_3 sample, obtained by the photodeposition method, the interfacial area between Pd and WO_3 was higher. Furthermore, the black light used for the photodeposition had an energy that greatly exceeded the bandgap of WO_3, which was 2.7–2.8 eV [18–21]. Therefore, it excited electrons not only at the top of the valence band of the O2p orbital but also at deeper levels. The fact that the excitation energy was far greater than the bandgap of WO_3 prevented the photoexcited electrons from recombining with holes; these electrons resulted in the reduction of Pd(II). Therefore, it can be assumed that most of the Pd distributed on the surface of WO_3 was reduced from a two-valence state to a zero-valence state, as it was photodeposited using black light.

Please cite this article in press as: Y. Sakai, et al., Fabrication of high-sensitivity palladium loaded tungsten trioxide photocatalyst by photodeposite method, Catal. Today (2014), http://dx.doi.org/10.1016/j.cattod.2014.07.044

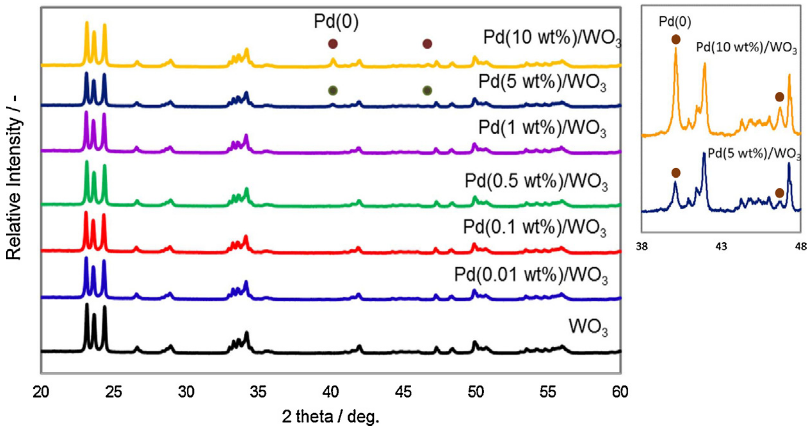

Fig. 2. XRD patterns of WO_3 and Pd/WO_3.

The UV–Visible absorption spectra of P25 (Degussa), WO_3, and the synthesized Pd/WO_3, obtained from their diffuse reflections, are shown in Fig. 4. The gray spectrum is attributable to P25 and the black spectrum to unsupported WO_3 [34,35]. Absorption in the long-wavelength region increased with the Pd addition ratio. It is believed that the absorption was owing to the surface plasmons attributable to Pd black in the form of Pd(0) [36]. Visible-light absorption increased markedly when the Pd addition ratio was 0.5 wt% or higher. This shows that the surface of WO_3 covered by Pd increased in area with an increase in the Pd addition ratio.

Fig. 5 shows the relationship between the visible-light (>417 nm) irradiation time and the absorbance during the degradation of aqueous MB. No discoloration of the MB solution was observed under these conditions when a photocatalyst was not used. The results obtained in the case of unsupported WO_3 and P25 were used as references. For all the samples, the MB solution underwent slight discoloration in the dark, owing to surface adsorption. The MB absorbance for each sample tended to decrease under visible-light irradiation. The first-order rate constant was determined from the curves shown in Fig. 5; it was assumed that the degradation reaction followed first-order kinetics after the samples had been irradiated. However, the MB concentration decreased with an increase in the irradiation time as well. This overall reaction is not a first-order one. Therefore, this calculation was performed only for the initial reaction rate, for which there was a large enough supply of MB.

The relationship between the Pd addition ratio and the first-order rate constant is shown in Fig. 6. The highest value of the first-order rate constant under visible-light irradiation was 0.59 h^{-1}, which corresponded to a Pd addition ratio of 0.5 wt%; this value was approximately 27 and 28 times higher than those for pure WO_3 and P25, respectively. When the Pd addition ratio was 0.5 wt% or lower, the photocatalytic activity increased with an increase in the ratio. We investigated MB degradation under a fluorescent lamp including UV rays as well; the relation between the addition ratio and the first-order rate constant was determined for this condition

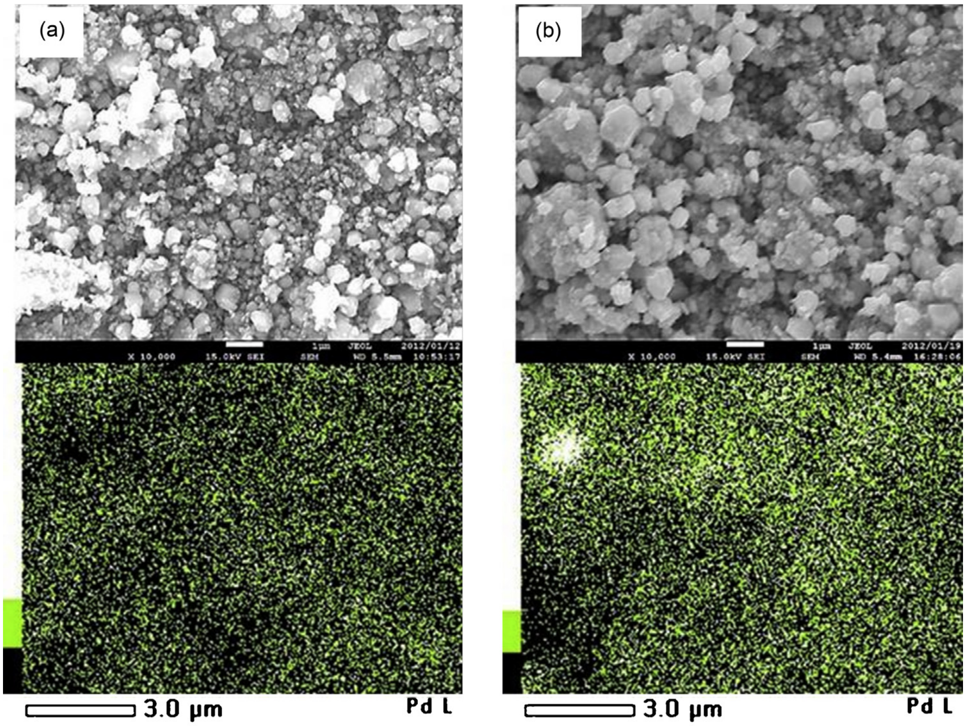

Fig. 3. FE-SEM images and the Pd elemental concentration maps for (a) Pd(0.5 wt%)/WO_3 and (b) Pd(5 wt%)/WO_3.

Please cite this article in press as: Y. Sakai, et al., Fabrication of high-sensitivity palladium loaded tungsten trioxide photocatalyst by photodeposite method, Catal. Today (2014), http://dx.doi.org/10.1016/j.cattod.2014.07.044

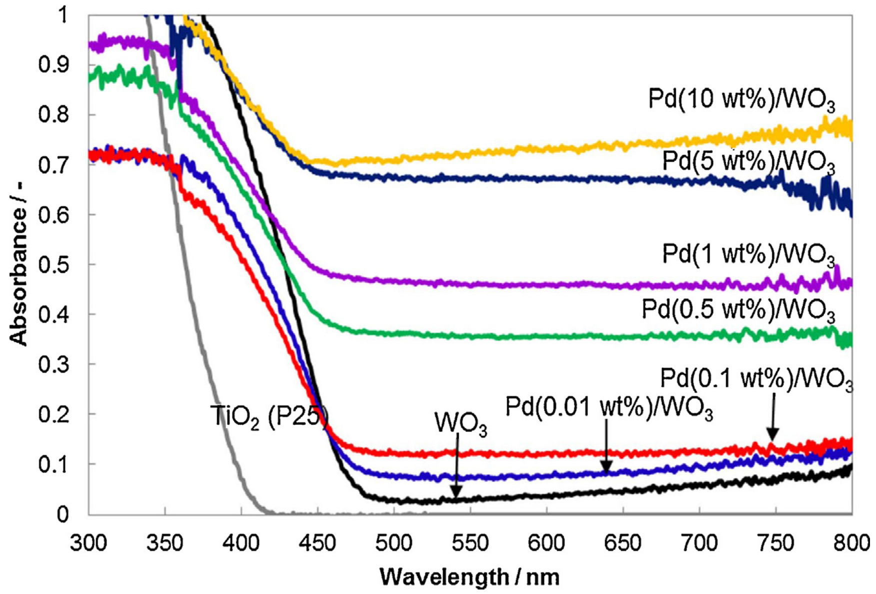

Fig. 4. UV–Visible absorption spectra of P25 (Degussa), WO_3, and the synthesized Pd/WO_3.

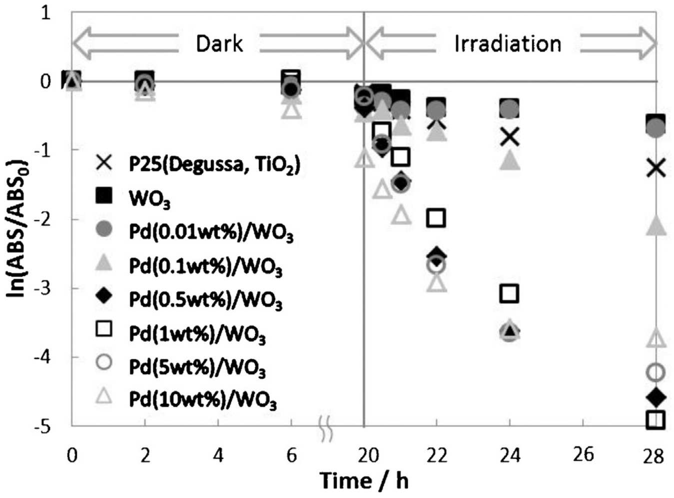

Fig. 5. Relationship between the visible-light (>417 nm) irradiation time and the absorbance during the degradation of aqueous MB.

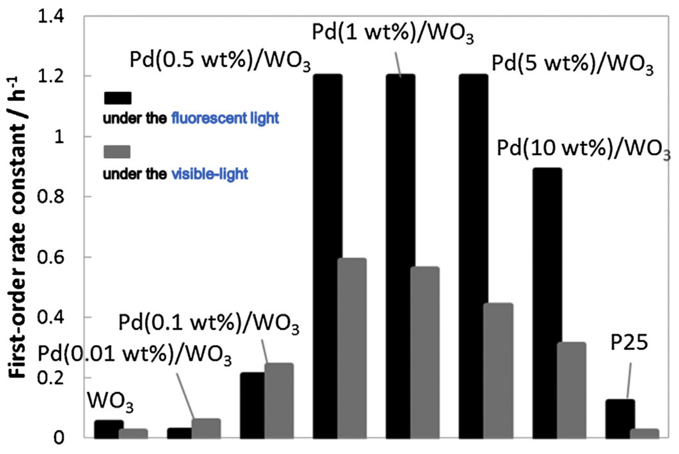

Fig. 6. Relationship between the Pd addition ratio and the first-order rate constant.

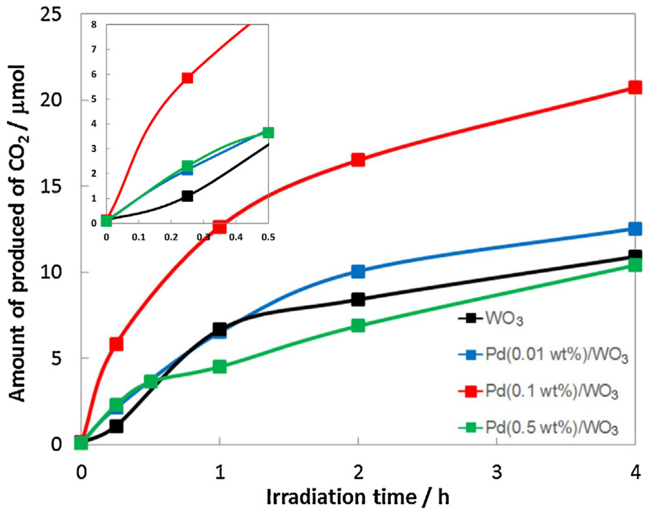

Fig. 7. Photocatalytic activities of the various samples during the decomposition of gaseous acetaldehyde.

too. Under fluorescent-lamp irradiation, the first-order rate constant for a Pd addition ratio of 0.1 wt% was approximately 7 times that in the case of unsupported WO_3. The highest value of the first-order rate constant under fluorescent-light irradiation was 1.2 h^{-1} and corresponded to a Pd addition ratio of 0.5 wt%; this value was approximately 23 and 10 times higher than those for pure WO_3 and P25, respectively.

Fig. 7 shows the photocatalytic activities of the various samples during the decomposition of gaseous acetaldehyde.

The relationship between the addition ratio and the initial CO_2 production rate is shown in Table 1 (the first 15 min of photoinduced degradation test). The highest value of the initial CO_2 production rate under visible-light irradiation was 22.8 $\mu mol\,h^{-1}$ and corresponded to a Pd addition ratio of 0.1 wt%; this value was approximately 5.9 times greater than that for pure WO_3. The top of the valence band of WO_3 is approximately at 3.2 eV. Therefore, the holes formed by photoexcitation have high oxidation power and are effective in decomposing organic matter. However, because the lower conductive area is approximately at +0.5 eV, it is thought

Please cite this article in press as: Y. Sakai, et al., Fabrication of high-sensitivity palladium loaded tungsten trioxide photocatalyst by photodeposite method, Catal. Today (2014), http://dx.doi.org/10.1016/j.cattod.2014.07.044

Table 1
Relationship between the Pd addition ratio and the initial CO_2 production rate.

Photocatalyst sample	Initial CO_2 production rate/μmol h^{-1}	The amount of CO_2 at 6 h/μmol
WO_3	3.85	10.9
Pd(0.01 wt%)/WO3	8.15	12.5
Pd(0.1 wt%)/WO3	22.8	20.7
Pd(0.5 wt%)/WO3	8.89	10.4

that, in the case of excited electrons, the reductive reaction does not occur readily [24,28].

Moreover, in the case of the WO_3-based photodecomposition of gaseous acetaldehyde, the initial reaction rate is high; however, WO_3 is covered by the intermediate acetic acid, formaldehyde and formic acid [28]. Therefore, it is highly likely that the reaction rate became extremely low.

It is known that, when used as a support, Pd induces a multielectron reduction reaction [23]. In the case of Pd/WO_3, the photoexcited electrons migrate to the Pd site. For these electrons, the degree of surface oxidation reduction is reduced, and, as a result, hydrogen peroxide is generated. Therefore, in the case of the Pd supporter, the efficiency of use of holes in Pd/WO_3 improves.

When zero-valence Pd is present in a large amount and when the Pd–WO_3 interfacial area is high, photoexcited electrons in the conduction band on the WO_3 side are transferred efficiently to the Pd side. It can be assumed that the increase in the charge separation efficiency owing to the use of Pd as a support is attributable to the increase in the efficiency of production of photoexcitation holes [30,37]. In addition, on the Pd side, the transferred electrons are likely to form superoxide anions on the surface, which results in the formation of hydrogen peroxide [30]. On the basis of the fact that hydrogen peroxide was shown to decompose MB under fluorescent light under the investigated test conditions, it can be assumed that the additional photoreactions that occur owing to the created hydrogen peroxide contribute to the fading. Moreover, holes with very high oxidizing power are generated by optical excitation at the oxygen sites, and these holes produce various activated species.

Because the light source used in this paper had an energy that exceeds the WO_3 energy gap, the following three reactions contributed to the color degradation of MB (dye).

[i] MB discolored owing to excitation by the light that it absorbed, resulting in the consumption of the excitation electrons on the Pd/WO_3 side; [ii] owing to the use of photoexcited electrons on the WO_3 side of the Pd side; and [iii] because of oxidation resulting from the holes generated by optical excitation [30].

In case of the decomposition of MB, the amount of Pd that shows high photocatalyst revitalization is the range of 0.5–5 wt%. This is because the reaction of [ii] and [iii] does not progress readily. On the other hand, it becomes easy for the reaction of [i] to progress because the rate at which Pd is coated on the surface of WO_3 increases when the amount of Pd is increased.

In case of acetaldehyde decomposition, the speed of the initial reaction is high, then the reaction rate thereafter decreases. The hole generated by the photoexcitation contributes to the organic matter decomposition, the excited electron migrates to the Pd side, and generates hydrogen peroxide.

The rate of generation of hole–electron pairs is determined by the amount of light used and by the number of excitation electrons that reach the surface of WO_3. Therefore, it is thought that the highest photocatalyst revitalization occurs when the consumption efficiency of the charge that moved to the generation efficiency and the Pd site of hole–electron pair who generates it by excitation are optimal balances. When the amount of Pd supported was 0.1 wt%, acetaldehyde decomposition exhibited the highest revitalization.

As mentioned above, because the response mechanisms for MB resolution and acetaldehyde resolution are different, the relation between the optimum amount of supported Pd and photocatalyst revitalization is different.

4. Conclusion

A high-performance visible-light-responsive photocatalyst, Pd/WO_3, was prepared by photodeposition under black light. The thus-synthesized Pd/WO_3 was found to contain a large amount of Pd(0). The results showed that Pd(0) can be distributed over the entire surface of WO_3 by ensuring that Pd(II) is reduced to a sufficient degree during photodeposition using black light. Under constant fluorescent-light or visible-light irradiation, the photocatalytic activity of WO_3, when supported by Pd in amounts of 0.1 wt% or greater, was higher those that of pure WO_3 and P25. The optimum addition ratio of Pd was determined to be 0.5 wt% for the degradation of aqueous methylene blue (the photocatalytic activity in this case was 27 times higher than that of pure WO_3) and 0.1 wt% for the decomposition of gaseous acetaldehyde (the photocatalytic activity in this case was 5.9 times higher than that of pure WO_3). Pd as a support served to improve the charge separation efficiency; in addition, hydrogen peroxide was produced on the Pd side of the photocatalyst. Further, MB discolored owing to excitation by the light that it absorbed, resulting in the consumption of the excitation electrons on the Pd/WO_3 side. Therefore, because the response mechanisms during MB resolution and acetaldehyde resolution were different, the relation between the optimum amount of supported Pd and photocatalyst revitalization is different.

Finally, it was confirmed that the Pd/WO_3 sample containing Pd in the optimal amount acted as an effective photocatalyst, even though there was a difference in the optimal amount of Pd for acetaldehyde decomposition and that for MB degradation.

Acknowledgments

This work was supported by industry to support private universities building up their foundations of strategic research from the Ministry of Education, Culture, Sports, Science and Technology (MEXT) of the Japanese Government.

References

[1] M.R. Hoffmann, S.T. Martin, W.Y. Choi, D.W. Bahnemann, Chem. Rev. 95 (1995) 69.
[2] G.-M. Zuo, Z.-X. Cheng, H. Chen, G.-W. Li, T. Miao, J. Hazard. Mater. B128 (2006) 158.
[3] M.N. Chong, B. Jin, C.W.K. Chow, C. Saint, Water Res. 44 (2010) 2997.
[4] T.E. Doll, F.H. Frimmel, Catal. Today 101 (2005) 195.
[5] K. Hashimoto, H. Irie, A. Fujishima, Jpn. J. Appl. Phys. 44 (2005) 8269.
[6] P. Mohapatra, T. Mishra, K.M. Parida, Appl. Catal. A: Gen. 310 (2006) 183.
[7] M. Anpo, M. Takeuchi, Int. J. Photoenergy 3 (2001) 89.
[8] T. Umebayashi, T. Yamaki, H. Itoh, K. Asai, J. Phys. Chem. Solids 63 (2002) 1909.
[9] R. Asahi, T. Morikawa, T. Ohwaki, K. Aoki, Y. Taga, Science 293 (2001) 269.
[10] H. Irie, Y. Watanabe, K. Hashimoto, J. Phys. Chem. B 107 (2003) 5483.
[11] H. Irie, S. Washizuka, Y. Watanabe, T. Kako, K. Hashimoto, J. Electrochem. Soc. 152 (2005) E351.
[12] T. Ohno, T. Mitsui, M. Matsumura, Chem. Lett. 32 (2003) 364.
[13] M. Mrowetz, W. Balcerski, M.R. Hoffmann, J. Phys. Chem. B 108 (2004) 17269.
[14] R. Nakamura, T. Tanaka, Y. Nakato, J. Phys. Chem. B 108 (2004) 10617.
[15] K.M. Parida, N. Sahu, J. Mol. Catal. A: Chem. 287 (2008) 161.
[16] B. Naik, K.M. Parida, Ind. Eng. Chem. Res. 49 (2010) 8339.
[17] S. Pany, K.M. Parida, B. Naik, RSC Adv. 3 (2013) 4976.
[18] G.R. Bamwenda, K. Sayama, H. Arakawa, J. Photochem. Photobiol. A 122 (1999) 175.
[19] M. Miyauchi, A.K. Nakajima, K. Hashimoto, T. Watanabe, Adv. Mater. 12 (2000) 1923.
[20] S. Higashimoto, M. Sakiyama, M. Azuma, Thin Solid Films 503 (2006) 201.
[21] T. Arai, M. Yanagida, Y. Konishi, Y. Iwasaki, H. Sugihara, K. Sayama, J. Phys. Chem. C 111 (2007) 7574.
[22] H. Irie, S. Miura, K. Kamiya, K. Hashimoto, Chem. Phys. Lett. 457 (2008) 202.
[23] R. Abe, H. Takami, N. Murakami, B. Ohtani, J. Am. Chem. Soc. 130 (2008) 7790.
[24] M. Miyauchi, Phys. Chem. Chem. Phys. 10 (2008) 6258.
[25] F. Yang, Y. Takahashi, N. Sakai, T. Tatsuma, J. Phys. Chem. C 115 (2011) 18270.

Please cite this article in press as: Y. Sakai, et al., Fabrication of high-sensitivity palladium loaded tungsten trioxide photocatalyst by photodeposite method, Catal. Today (2014), http://dx.doi.org/10.1016/j.cattod.2014.07.044

[26] J. Kim, C.W. Lee, W. Choi, Environ. Sci. Technol. 44 (2010) 6849.
[27] T. Arai, M. Horiguchi, M. Yanagida, T. Gunji, H. Sugihara, K. Sayama, Chem. Commun. 43 (2008) 5565.
[28] T. Arai, M. Horiguchi, M. Yanagida, T. Gunji, H. Sugihara, K. Sayama, J. Phys. Chem. C 113 (2009) 6602.
[29] T. Arai, M. Yanagida, Y. Konishi, A. Ikura, Y. Iwasaki, H. Sugihara, K. Sayama, Appl. Catal. B: Environ. 84 (2008) 42.
[30] Y. Liu, Y. Ohko, R. Zhang, Y. Yang, Z. Zhang, J. Hazard. Mater. 184 (2010) 386.
[31] H.W. Choia, E.J. Kimb, S.H. Hahna, Chem. Eng. J. 161 (2010) 285.
[32] N. Le Houx, G. Pourroy, F. Camerel, M. Comet, D. Spitzer, J. Phys. Chem. C 114 (2010) 155.
[33] G.R. Bamwenda, H. Arakawa, Appl. Catal. A: Gen. 210 (2001) 181.
[34] M. Miyauchi, A.K. Nakajima, T. Watanabe, K. Hashimoto, Chem. Mater. 14 (2002) 2812.
[35] M. Miyauchi, A.K. Nakajima, T. Watanabe, K. Hashimoto, Chem. Mater. 14 (2002) 4714.
[36] M. Shibuya, M. Miyauchi, Adv. Mater. 21 (2009) 1373.
[37] Y.L. Liu, L.J. Guo, W. Yan, H.T. Liu, J. Power Sources 159 (2006) 1300.

Please cite this article in press as: Y. Sakai, et al., Fabrication of high-sensitivity palladium loaded tungsten trioxide photocatalyst by photodeposite method, Catal. Today (2014), http://dx.doi.org/10.1016/j.cattod.2014.07.044